The Astrophysical Journal, 585:767–774, 2003 March 10

EVIDENCE FOR AN INTERMEDIATE-AGE, METAL-RICH POPULATION OF GLOBULAR CLUSTERS IN NGC 4365[1]

Søren S. Larsen and Jean P. Brodie
University of California Observatories/Lick Observatory, Santa Cruz, CA 95064;
soeren@ucolick.org, brodie@ucolick.org

Michael A. Beasley and Duncan A. Forbes
Centre for Astrophysics and Supercomputing, Swinburne University, Hawthorn VIC 3122, Australia;
dforbes@astro.swin.edu.au, mbeasley@astro.swin.edu.au

Markus Kissler-Patig and Harald Kuntschner
European Southern Observatory, Karl-Schwarzschild-Straße 2, D-85748 Garching, Munich, Germany;
mkissler@eso.org, hkuntsch@eso.org

and

Thomas H. Puzia
Sternwarte München, Scheinerstrasse 1, D-81679 Munich, Germany; puzia@usm.uni-muenchen.de
Received 2002 July 24; accepted 2002 November 20

ABSTRACT

We present spectroscopy for globular clusters (GCs) in the elliptical galaxy NGC 4365, obtained with the Low-Resolution Imaging Spectrograph on the Keck I telescope. Previous studies have shown that the optical color distribution of GCs in NGC 4365 lacks the bimodal structure that is common in globular cluster systems, showing only a single broad peak. Measurements of Balmer line indices (Hβ, Hγ, and Hδ) on the GC spectra support recent suggestions by Puzia et al. on the basis of optical and near-infrared photometry that some of the clusters in NGC 4365 are intermediate-age (2–5 Gyr) and metal-rich ($-0.4 \lesssim [Z/H] \lesssim 0$) rather than old ($\sim$10–15 Gyr) and metal-poor. We also find some genuinely metal-poor, old clusters, suggesting that the ages and metallicities of the two populations conspire to produce the single broad distribution observed in optical colors.

Subject headings: galaxies: elliptical and lenticular, cD — galaxies: evolution — galaxies: individual (NGC 4365) — globular clusters: general

1. INTRODUCTION

Several recent studies have shown that complicated color distributions in globular cluster systems (GCSs) are the norm rather than the exception (Gebhardt & Kissler-Patig 1999; Kundu & Whitmore 2001; Larsen et al. 2001). In many cases, the GCS color distributions can be fairly well modeled as a superposition of two Gaussians with peaks at $(V-I)_0 \approx 0.95$ and $(V-I)_0 \approx 1.18$. These colors correspond to mean metallicities of $[Z/H] = -1.4$ and $[Z/H] = -0.6$ (Kissler-Patig et al. 1998) if both populations are old, i.e., they have similar ages (10–15 Gyr) as those in the Milky Way.

Although the color differences of globular clusters have been generally assumed to be mainly a function of metallicity, it is clear that age differences between GC subpopulations will also affect their colors, making a younger population appear bluer for a given metallicity. There are a few cases in which only a single, broad peak is observed in the optical GC color distribution, usually at blue or intermediate colors. While these systems simply might lack a distinct metal-rich component that would normally show up as the red peak, another interesting possibility is that the metal-rich population is indeed present but has a significantly lower age than the metal-poor one, shifting it to bluer colors and making the two populations appear as a single broad peak in optical colors. Using optical photometry alone, this degeneracy between age and metallicity cannot be easily broken, and alternative methods are needed to provide independent constraints on metallicity or age (or both).

Combining optical and near-infrared imaging of GCs in the $\sim$3 Gyr old merger remnant NGC 1316, Goudfrooij et al. (2001) have recently demonstrated that an old, metal-poor population and a very metal-rich, younger population with an estimated age consistent with that of the merger (Kuntschner & Davies 1998) masquerade as a single peak in optical colors. It is possible that other systems with an apparently unimodal GC color distribution might in a similar way be composed of several populations with large age differences.

The giant elliptical galaxy NGC 4365 at the outskirts of the Virgo Cluster is another example of a galaxy with only a single broad peak in the GC $V-I$ color distribution (Forbes et al. 1996; Gebhardt & Kissler-Patig 1999; Larsen et al. 2001). From optical and near-infrared photometry, Puzia et al. (2002, hereafter P02) have suggested that some of the GCs in NGC 4365 indeed might be intermediate-age (2–8 Gyr) and very metal-rich ($Z_\odot$–3 $Z_\odot$). In this paper, we use new spectroscopic data to further investigate the ages and metallicities of GCs in NGC 4365.

2. DATA

Spectra for GC candidates in NGC 4365 were obtained in multislit mode on 2002 February 9 and February 10 with the Low-Resolution Imaging Spectrograph (LRIS)

[1] Based on data obtained at the W. M. Keck Observatory, which is operated as a scientific partnership among the California Institute of Technology, the University of California, and the National Aeronautics and Space Administration.

(Oke et al. 1995) on the Keck I telescope. Candidate young clusters were selected from the data in P02, but to fill up the slit mask, a number of objects without *K*-band imaging were also included. We obtained nine exposures with integration times of 30–60 minutes, yielding a total exposure time of 390 minutes (6.5 hr). Observations were carried out simultaneously with the blue and red sides on LRIS, using a dichroic splitting at 5600 Å. On the blue side, we used a 600 line mm^{-1} grism, covering 3800–5600 Å, while a 600 line mm^{-1} grating blazed at 5000 Å was used on the red side, covering the range 5600–7900 Å. A number of radial velocity and flux standards, as well as Lick/IDS standard stars from Worthey et al. (1994) were also observed. The radial velocity standards were picked from the compilation in Barbier-Brossat & Figon (2000; stars 9934 and 10927), while the flux standards were PG 0934+554 and Hiltner 600 (Massey et al. 1988). Because the spectral range covered in long-slit mode is slightly different from the one covered in multislit mode, we observed the flux standards in multislit mode through one of the slitlets in the NGC 4365 slit mask to facilitate flux calibration over the entire spectral range of the science spectra. A slit width of 1″.0 was used for all observations.

Initial processing of the images (bias subtraction, flat-field correction, cosmic-ray removal, etc.) was done with standard tools in IRAF.[2] After correction for optical distortions, each individual spectrum was extracted using the APALL task in the SPECRED package in IRAF. Following wavelength calibration based on arc lamps mounted within the spectrograph, small zero-point corrections (1–3 Å) were applied by measuring the [O I] skylines at 5577.338 Å (blue spectra) and 6300.304 Å (red spectra). Finally, flux calibration was applied, and the individual spectra of each object were summed. Three sample spectra are shown in Figure 1.

Basic data for the cluster candidates are listed in Table 1. The V, I photometry is from the *Hubble Space Telescope* (*HST*) data used in Larsen et al. (2001), while the *K* magnitudes are from the VLT/Infrared Spectrometer and Array Camera (ISAAC) data in P02. Radial velocities were determined by cross-correlating the cluster spectra with those of the radial velocity (RV) standards using the FXCOR task in the RV package in IRAF. The radial velocities listed in Table 1 are an average of the cross-correlation results for each reference star, where the errors are estimates of the standard error on the mean based on the two measurements. We note that there is a systematic difference of about 100 km s^{-1} between the radial velocity measurements for each of the two stars, suggesting that the cataloged velocity of at least one of the stars is erroneous or that one star might have been misidentified. If this systematic difference is taken into account, the rms difference between the two sets of measurements is only about 13 km s^{-1}, so the relative radial velocities are probably more accurate than implied by the errors listed in Table 1. For NGC 4365 itself, the RC3 catalog (de Vaucouleurs et al. 1991) lists a radial velocity of 1243 ± 6 km s^{-1}. Four objects turned out to either be likely foreground stars or have too low a signal-to-noise ratio (S/N) to extract a useful spectrum. This leaves us with 14 confirmed clusters, with a mean radial velocity of 1144 ± 75 km s^{-1} and a dispersion of 279 ± 67 km s^{-1}.

[2] IRAF is distributed by the National Optical Astronomical Observatory, which is operated by the Association of Universities for Research in Astronomy, Inc., under contract with the National Science Foundation.

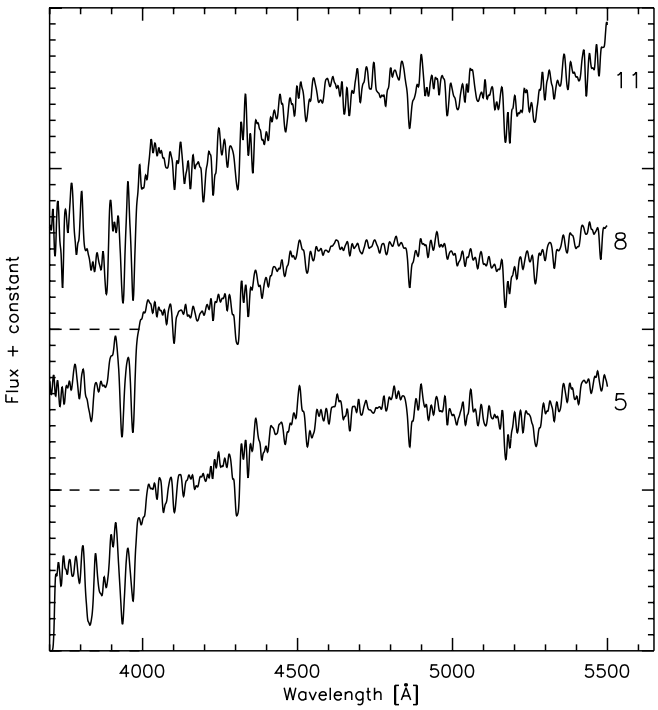

FIG. 1.—Three sample spectra, smoothed to the Lick/IDS resolution. The spectra have been shifted to 0 radial velocity. *Short-dashed lines*: Offsets have been added to the intensity scales of objects 8 and 11 for clarity.

3. MEASURING LICK/IDS INDICES

In order to estimate ages and metallicities for the GCs, we employ the Lick/IDS system of absorption indices (Worthey et al. 1994), including $H\delta_A$ and $H\gamma_A$ from Worthey & Ottaviani (1997). After correcting for the radial velocities in Table 1, we remeasured the locations of several prominent features such as the Balmer lines, G band, and Ca II H+K lines and found the wavelength scales to be accurate to better than 1 Å in the relevant range (i.e., ~4000–5500 Å). Because our LRIS spectra have a higher spectral resolution (~5 Å FWHM) than the original Lick/IDS system (8–13 Å), we smoothed our spectra to the IDS resolution with a wavelength-dependent Gaussian kernel before measuring the indices. Another difference between the original Lick/IDS system and our LRIS spectra is the fact that we are working on flux-calibrated data, whereas the original Lick/IDS spectra on which the Lick system is based were not flux calibrated. However, it is well documented that differences in flux-calibration procedures affect the equivalent widths of most Lick indices only weakly at the level of $\lesssim 0.1$ Å (Faber et al. 1985; Kissler-Patig et al. 1998; Larsen & Brodie 2002). One possible exception is the Mg_2 index, whose continuum passbands are more widely separated and where offsets between instrumental systems and the Lick standard system have often been found (Kuntschner 2000).

For most indices, we were able to check the agreement between our instrumental system and the Lick standard system using the Lick/IDS standard star observations. Figure 2 shows our standard star measurements versus the standard values (Worthey et al. 1994; Worthey & Ottaviani

TABLE 1
GLOBULAR CLUSTER CANDIDATES IN NGC 4365

IDENTIFICATION	COORDINATES (J2000.0) R. A.[a]	Decl.[a]	*HST*/WFPC2 V	$V-I$	VLT/ISAAC K	RV (km s^{-1})	GLOBULAR CLUSTER?
1	12 24 24.083	07 17 44.31	21.98 ± 0.01	1.090 ± 0.010	...	1265 ± 52	Yes
2	12 24 25.470	07 17 54.55	22.38 ± 0.02	0.898 ± 0.027	...	1428 ± 56	Yes
3	12 24 25.672	07 18 01.30	22.20 ± 0.02	0.892 ± 0.024	...	1177 ± 62	Yes
4	12 24 24.311	07 18 25.50	22.06 ± 0.01	0.987 ± 0.020	19.44 ± 0.07	1248 ± 58	Yes
5	12 24 25.298	07 18 25.61	21.27 ± 0.01	1.089 ± 0.011	18.52 ± 0.04	1628 ± 54	Yes
6	12 24 24.718	07 18 58.99	22.48 ± 0.02	0.582 ± 0.036	...	136 ± 58	No
7	12 24 26.654	07 18 55.14	22.02 ± 0.02	1.015 ± 0.029	18.88 ± 0.05	362 ± 228	?
8	12 24 26.636	07 19 09.36	20.13 ± 0.01	1.029 ± 0.006	17.35 ± 0.02	1001 ± 19	Yes
9	12 24 25.914	07 19 34.58	21.57 ± 0.01	1.063 ± 0.013	18.68 ± 0.04	875 ± 56	Yes
10	12 24 29.465	07 19 03.49	22.62 ± 0.02	0.701 ± 0.038	...	...	?
11	12 24 27.425	07 19 42.22	22.17 ± 0.02	1.105 ± 0.024	19.24 ± 0.06	514 ± 49	Yes
12	12 24 28.724	07 19 38.26	21.45 ± 0.01	1.028 ± 0.016	18.69 ± 0.04	1302 ± 28	Yes
13	12 24 29.409	07 19 50.07	21.60 ± 0.01	1.032 ± 0.016	18.77 ± 0.04	1115 ± 43	Yes
14	12 24 28.595	07 20 08.39	21.63 ± 0.01	1.141 ± 0.013	18.51 ± 0.04	1395 ± 40	Yes
15	12 24 30.330	07 20 04.26	21.64 ± 0.01	1.033 ± 0.015	18.89 ± 0.05	1003 ± 35	Yes
16	12 24 29.409	07 21 35.16	21.33 ± 0.01	1.128 ± 0.009	...	1188 ± 40	Yes
17	12 24 28.869	07 21 57.34	20.56 ± 0.01	1.185 ± 0.006	...	880 ± 48	Yes
18	12 24 31.509	07 22 32.15	21.59 ± 0.01	0.825 ± 0.013	...	191 ± 31	No

NOTE.—No correction for Galactic foreground reddening has been applied to the photometry in this table. Coordinates are measured on the WFPC2 images.

[a] Right ascension is given in hours, minutes, and seconds. Declination is given in degrees, arcminutes, and arcseconds.

1997). The mean offsets are listed in Table 2. Even after smoothing, systematic offsets of 0.1–0.2 Å remained between our measurements and the standard values. Unfortunately, since the Lick/IDS standard stars were observed in long-slit mode, they did not include the red continuum passbands of Mg_2 and Fe 5335, so we were unable to check these two indices. Because some of the indices fell outside the spectral range of the standard star observations

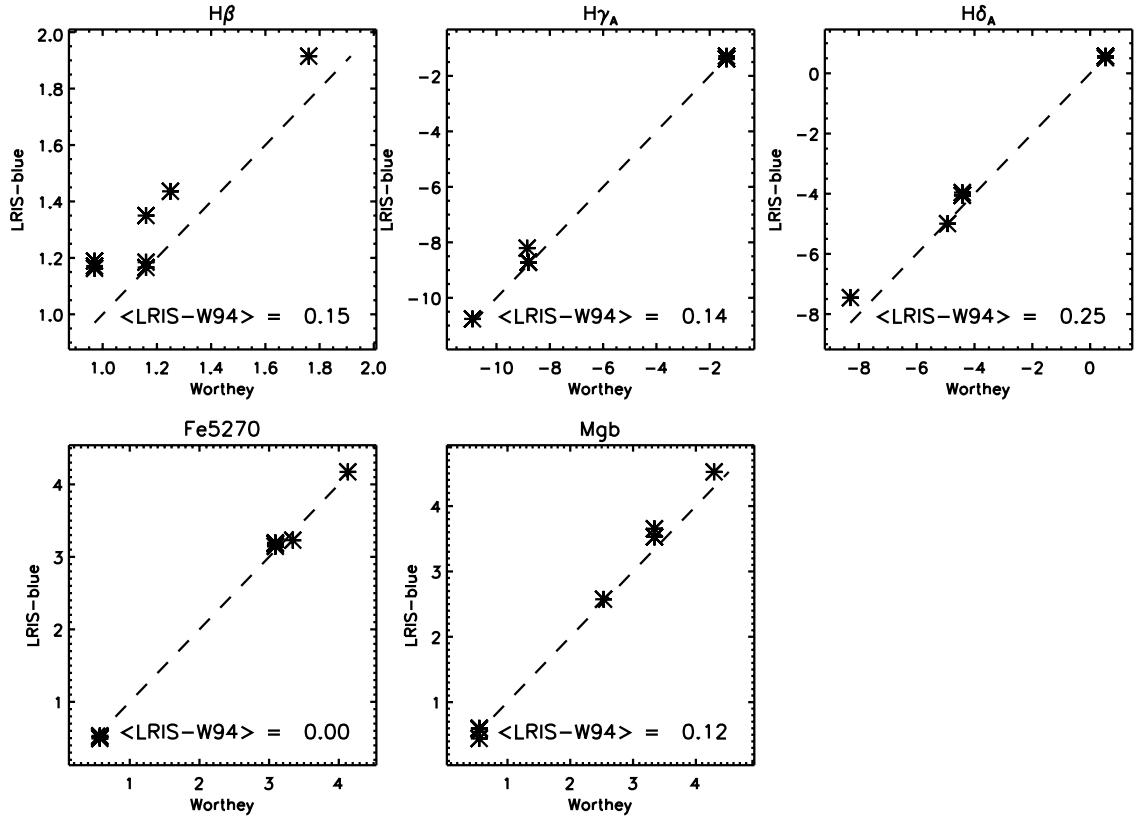

FIG. 2.—Comparison of our Lick/IDS index measurements for the standard stars and the Worthey et al. (1994) standard values

TABLE 2
OFFSETS BETWEEN OUR STANDARD STAR MEASUREMENTS AND VALUES TABULATED BY WORTHEY ET AL. (1994) AND WORTHEY & OTTAVIANI (1997)

Index	⟨Measured−Standard⟩ (Å)
Hβ	0.15 ± 0.03
Hγ_A	0.14 ± 0.07
Hδ_A	0.25 ± 0.11
Fe 5270	0.00 ± 0.03
Mg b	0.12 ± 0.05

and some of the globular cluster spectra have measured indices outside the range spanned by the standard stars, we have not attempted to correct our index measurements on the science spectra for the offsets between our instrumental system and the Lick/IDS standard system. However, we note that these small offsets are of no consequence to our analysis or conclusions and are generally smaller than the random measurement errors and model uncertainties. The indices used in this paper are listed in Table 3.

4. RESULTS

4.1. *Ages and Metallicities*

Figure 3 shows a (V–K, V–I) two-color diagram for GC candidates in NGC 4365 on the basis of the data in P02. The photometry has been corrected for a foreground reddening of $A_B = 0.091$ mag (Schlegel, Finkbeiner, & Davis 1998), adopting the extinction curve in Cardelli, Clayton, & Mathis (1989). The nine spectroscopically confirmed clusters with K-band data are shown with filled circles. Also shown are single-aged stellar population (SSP) models by C. Maraston (2003, in preparation) for ages of 2, 3, 4, 5, 6, 8, 11, and 14 Gyr and metallicities of $[Z/H] = -2.25$, -1.35, -0.33, 0.0, and $+0.35$. From the optical colors alone and assuming old ages, the nine clusters would appear to have low-to-intermediate metallicities, but their location in the two-color diagram suggests that they may instead be as young as 2–3 Gyr and have metallicities near solar. For a more detailed discussion of the (V–K, V–I) diagram, including a comparison of various SSP models, we refer to P02.

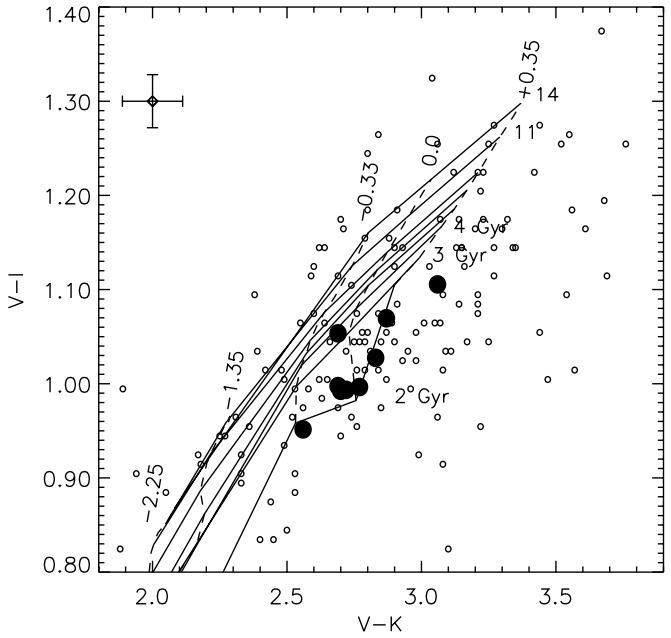

FIG. 3.—(V–K, V–I) two-color diagram for globular clusters in NGC 4365, shown together with a Maraston model grid. *Filled circles*: Nine clusters selected for spectroscopy. *Open circles*: Full sample from Puzia et al. (2002). A typical error bar is also shown.

In Figure 4, we show the Balmer line indices (Hβ, Hγ_A, and Hδ_A) for the clusters versus [MgFe] and ⟨Fe⟩, compared with SSP model grids by Thomas, Maraston, & Bender (2002, hereafter TMB02). A variety of SSP models are now available in the literature, but for this work, we have chosen the models by TMB02 because they are tabulated for several different [α/Fe] values and thus allow us to quantify the effect of varying α-element abundances. These models are also the first to attempt a correction for the [α/Fe] bias in the original Lick/IDS fitting functions (Maraston et al. 2002). We have used the common definitions $\langle Fe \rangle = (Fe\ 5270 + Fe\ 5335)/2$

TABLE 3
LICK/IDS INDICES FOR GLOBULAR CLUSTERS IN NGC 4365

Identification	Hβ (Å)	Hγ_A (Å)	Hδ_A (Å)	Fe 5270 (Å)	Fe 5335 (Å)	Mg_2 (mag)	Mg b (Å)	⟨Fe⟩ (Å)	[MgFe] (Å)
1	1.83 ± 0.41	-4.33 ± 0.66	-1.96 ± 0.79	1.67 ± 0.43	1.85 ± 0.48	0.271 ± 0.013	4.65 ± 0.43	1.76 ± 0.32	2.86 ± 0.29
2	1.96 ± 0.80	1.52 ± 0.96	3.32 ± 1.15	2.94 ± 0.88	2.19 ± 1.04	0.121 ± 0.020	0.81 ± 0.79	2.56 ± 0.68	1.44 ± 0.73
3	0.91 ± 0.65	0.26 ± 0.76	3.97 ± 1.02	1.13 ± 0.65	-0.49 ± 0.77	0.068 ± 0.015	-1.77 ± 0.69	0.32 ± 0.50	0.00 ± 0.85
4	1.50 ± 0.44	-1.18 ± 0.62	3.35 ± 0.61	1.72 ± 0.53	0.63 ± 0.63	0.115 ± 0.013	1.23 ± 0.50	1.17 ± 0.41	1.20 ± 0.32
5	2.65 ± 0.27	-3.99 ± 0.41	0.07 ± 0.55	3.12 ± 0.30	1.74 ± 0.38	0.144 ± 0.008	2.75 ± 0.28	2.43 ± 0.24	2.58 ± 0.18
8	2.03 ± 0.11	-2.79 ± 0.17	1.23 ± 0.20	1.90 ± 0.12	1.64 ± 0.15	0.175 ± 0.003	2.73 ± 0.12	1.77 ± 0.09	2.20 ± 0.08
9	2.58 ± 0.29	-2.03 ± 0.44	1.59 ± 0.58	2.18 ± 0.38	2.24 ± 0.52	0.162 ± 0.009	2.71 ± 0.32	2.21 ± 0.32	2.45 ± 0.23
11	3.01 ± 0.53	-2.75 ± 0.83	-0.14 ± 1.01	2.72 ± 0.61	2.67 ± 0.78	0.176 ± 0.017	3.16 ± 0.57	2.69 ± 0.50	2.92 ± 0.38
12	2.32 ± 0.34	-3.60 ± 0.47	0.79 ± 0.56	0.87 ± 0.35	1.39 ± 0.43	0.148 ± 0.010	2.54 ± 0.36	1.13 ± 0.28	1.69 ± 0.24
13	2.33 ± 0.40	-2.36 ± 0.61	1.17 ± 0.73	1.95 ± 0.46	1.92 ± 0.61	0.173 ± 0.011	2.88 ± 0.48	1.93 ± 0.38	2.36 ± 0.31
14	2.15 ± 0.36	-5.58 ± 0.58	-1.85 ± 0.72	3.18 ± 0.40	1.57 ± 0.49	0.243 ± 0.011	3.95 ± 0.39	2.37 ± 0.32	3.06 ± 0.25
15	2.31 ± 0.30	-2.53 ± 0.44	1.52 ± 0.48	2.91 ± 0.31	1.80 ± 0.42	0.201 ± 0.009	3.09 ± 0.33	2.36 ± 0.26	2.70 ± 0.21
16	1.79 ± 0.33	-3.37 ± 0.46	-1.14 ± 0.52	2.74 ± 0.37	1.25 ± 0.55	0.168 ± 0.010	1.89 ± 0.38	2.00 ± 0.33	1.94 ± 0.25
17	1.54 ± 0.17	-4.56 ± 0.25	-0.29 ± 0.32	...	...	...	...	...	...

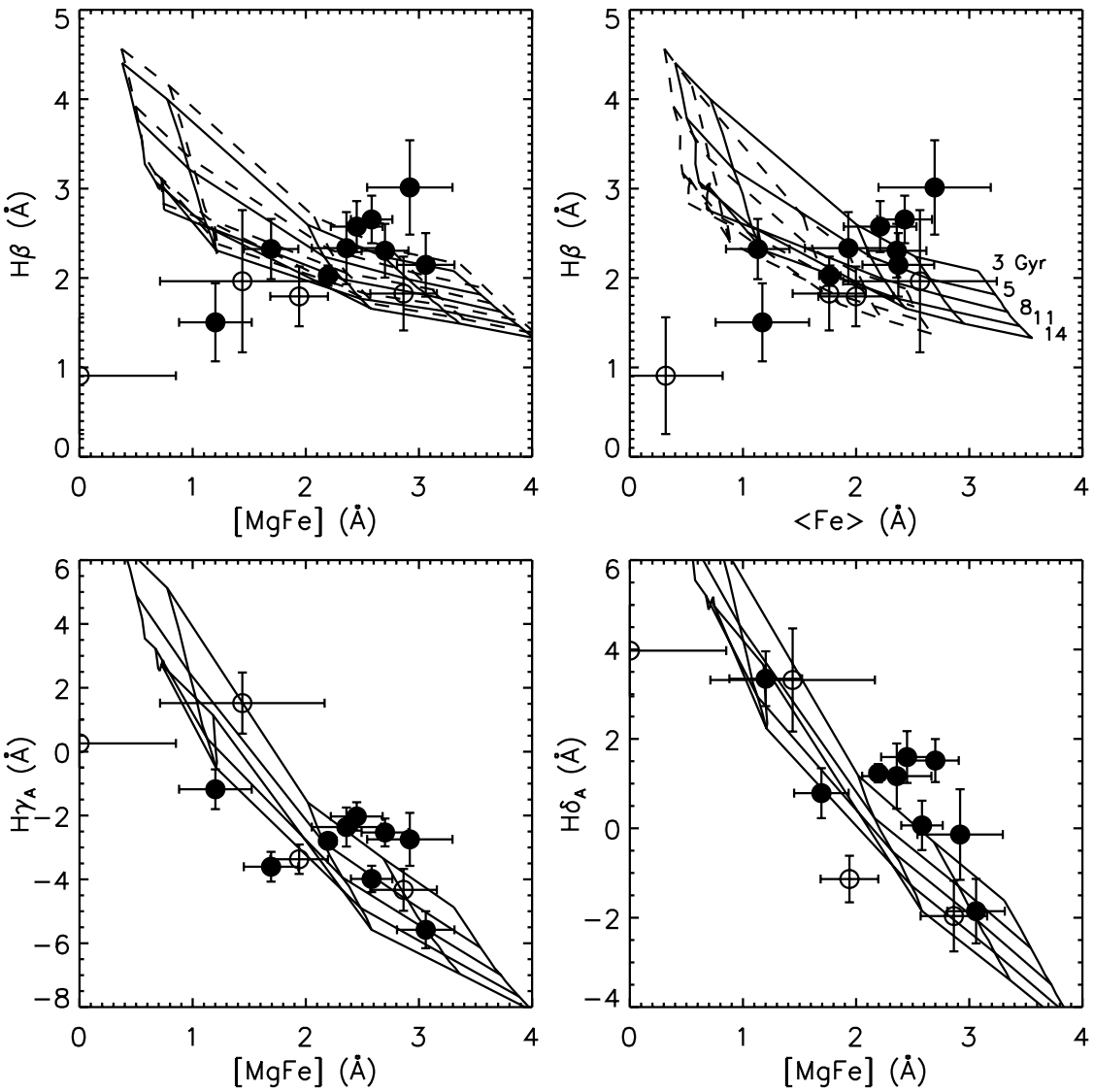

FIG. 4.—Comparison of index measurements for GCs in NGC 4365 with model grids from TMB02. The models are shown for ages of 3, 5, 8, 11, and 14 Gyr and mean metallicities $[Z/H] = -2.25, -1.35, -0.33, 0.0$, and $+0.35$. *Filled circles*: Clusters with *K*-band data. *Open circles*: Clusters without *K*-band data. *Top panels, solid and dashed-line grids*: $[\alpha/Fe] = 0$ and $[\alpha/Fe] = +0.5$.

and $[MgFe] = (Mgb\ \langle Fe\rangle)^{1/2}$ (González 1993). The SSP models are shown for ages of 3, 5, 8, 11, and 14 Gyr and the same metallicities as in Figure 3. In the plots involving Hβ, we show models with $[\alpha/Fe] = 0$ (*solid lines*) and $[\alpha/Fe] = +0.5$ (*dashed lines*). In the other plots, only $[\alpha/Fe] = 0$ models are shown. Clusters with and without *K*-band imaging are shown with filled and open circles, respectively. Object 3, which has Mg $b < 0$, is shown at $[MgFe] = 0$. The blue color of this cluster as well as its weak Fe indices suggest that it is very metal-poor. It is also one of the faintest objects in our sample and was observed in a short (6″) slit, making accurate sky subtraction difficult. The negative Mg *b* value is most likely due to contamination by the [N I] night-sky line at 5199 Å, which is shifted into the Mg *b* central bandpass after correcting for the radial velocity of NGC 4365.

All four panels in Figure 4 confirm a spread in metallicity, with some clusters approaching solar values, but none of the clusters included in our small sample appear to have metallicities significantly above solar. The combined $\langle Fe\rangle$ index measures primarily Fe-peak elements (Tripicco & Bell 1995) and is therefore sensitive to $[\alpha/Fe]$ when plotted for a fixed mean metallicity $[Z/H]$. The [MgFe] grids, on the other hand, vary only weakly with $[\alpha/Fe]$ for fixed $[Z/H]$, as can be seen from the similarity between the dashed-line and solid-line grids in the upper left panel of Figure 4. Comparison of Balmer line indices with the models again indicates intermediate ages for many of the metal-rich clusters, but note that some of the filled circles (all of which, by selection, appear young in Fig. 3) are actually better fit by the models corresponding to old ages. Thus, there are a few cases in which the spectroscopic and photometric data are not entirely consistent. Some of the clusters without infrared data also appear to be genuinely old.

The TMB02 models, like most other available SSP models, are based on the Lick/IDS fitting functions. A new set of SSP models based on fitting functions derived from the spectral library by Jones (1999) has recently been computed

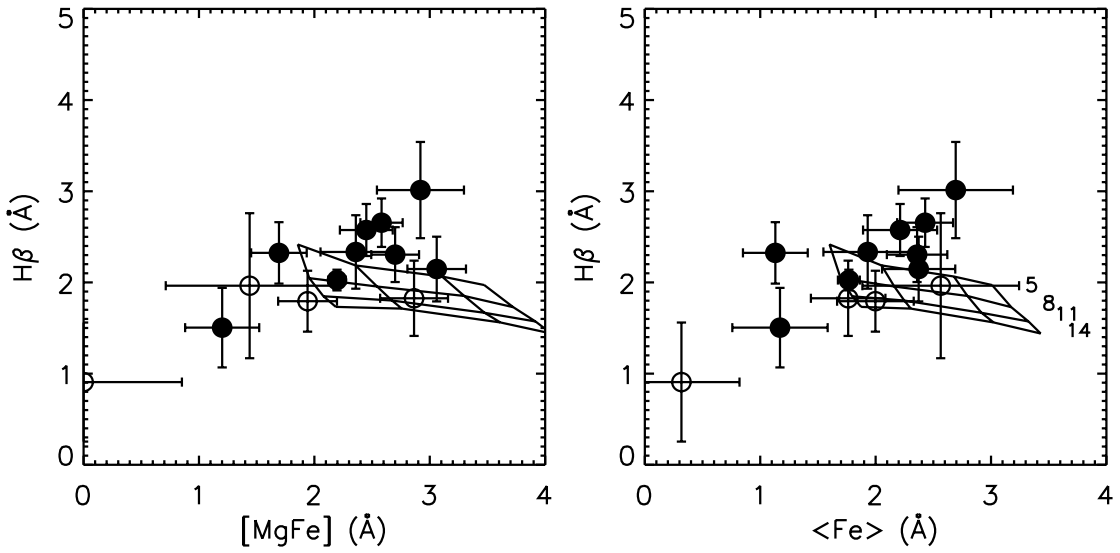

FIG. 5.—Comparison of index measurements for GCs in NGC 4365 with model grids from Schiavon (2002). The models are tabulated for ages of 5, 7.9, 11.2, and 14.1 Gyr and metallicities of $[Z/H] = -0.7, -0.4, 0.0$, and $+0.2$. Note the more restricted age and metallicity range compared to the TMB02 models. Symbols are the same as in Fig. 4.

by R. Schiavon and was kindly made available to us. (A discussion of some of the ingredients in these models is given in Schiavon et al. 2002.) The Schiavon models cover a more restricted range in age and metallicity but are useful as a comparison with the Maraston models. In Figure 5, we compare our measurements of Hβ, [MgFe], and $\langle$Fe$\rangle$ with the Schiavon models (based on Salaris isochrones). The slope of the lines of constant age in the Hβ versus [MgFe] and $\langle$Fe$\rangle$ planes differs somewhat from that in Figure 4, suggesting that even relative ages based on Balmer line indices may still be inherently uncertain at the level of a few gigayears. Nevertheless, the picture remains clear: many of the metal-rich clusters in NGC 4365 have stronger Hβ indices than even the 5 Gyr models and thus appear to be young.

Considering the current model uncertainties and observational errors, it is probably not very meaningful to assign absolute ages to any individual clusters, but Figures 3–5 consistently suggest that NGC 4365 hosts a substantial number of clusters as young as 2–5 Gyr and with near-solar metallicities. However, confirmation of this result with a larger sample of high S/N spectra clearly would be very desirable. We also note that factors such as horizontal branch morphology and the luminosity function on the red and asymptotic giant branches may affect line indices and remain major uncertainties in SSP models (Schiavon et al. 2002). This might account for some of the differences between the spectroscopic and photometric age/metallicity estimates and could also have a significant effect on ages derived from Balmer lines (Lee, Lee, & Gibson 2002).

4.2. [α/Fe] *Abundance Ratios*

In Figure 6, we compare our measurements of Mg_2 and Mg b (both indicators of α elements) with the SSP models by TMB02. We show the $[\alpha/Fe] = 0$ models for both 3 and 12 Gyr to illustrate that the relation between Mg_2 /Mg b and $\langle$Fe$\rangle$ is only expected to depend weakly on age. For the most metal-poor clusters, neither plot provides strong constraints on [α/Fe] ratios, although the Mg_2 versus $\langle$Fe$\rangle$ plot (which has the smallest formal errors) suggests supersolar [α/Fe] as in other old stellar populations. There may be a slight tendency for the most metal-rich clusters to have [α/Fe] closer to solar. While offsets may be present between our instrumental system and the Lick standard system for the Mg_2 index, comparison of the two panels in Figure 6 suggests that any such offset is relatively small. Ratios of [α/Fe] of $\approx+0.3$ are common in globular clusters and elliptical galaxies and are usually attributed to rapid, early enrichment dominated by Type II supernovae. For an intermediate-age population, one would expect the [α/Fe] ratios to be closer to solar since the gas would have been enriched with Fe-group elements by Type Ia supernovae over several gigayears (Thomas, Greggio, & Bender 1999). Thus, the trends in [α/Fe] with metallicity suggested by Figure 6 are again consistent with many of the metal-rich clusters being of intermediate age.

5. ORIGIN OF THE INTERMEDIATE-AGE POPULATION

The photometric optical/infrared and spectroscopic data clearly hint at an intermediate-age, metal-rich population of GCs in NGC 4365. Although we would expect the globular cluster populations to trace major star formation episodes in their host galaxy, little is currently known about the detailed star formation history of any elliptical galaxy, and NGC 4365 is no exception. Based on a comparison of Hβ, $\langle$Fe$\rangle$, and Mg_2 measurements with a 1992 version of the Worthey SSP models combined with kinematic evidence, Surma & Bender (1995) suggested that a metal-rich (up to 2 $Z_\odot$) and $\sim$7 Gyr old stellar population with a mass of $(8.1 \pm 2.5) \times 10^9\ M_\odot$ exists in the central regions of NGC 4365. However, new results from integral field spectroscopy of NGC 4365 (Davies et al. 2001) and comparison with more recent SSP models indicate a luminosity-weighted age for the stellar population in the galaxy of about 14 Gyr over a continuous central region covering 0.5 effective radii. NGC 4365 does not show any of the usual signs of merger activity within the last few gigayears (H I tidal tails,

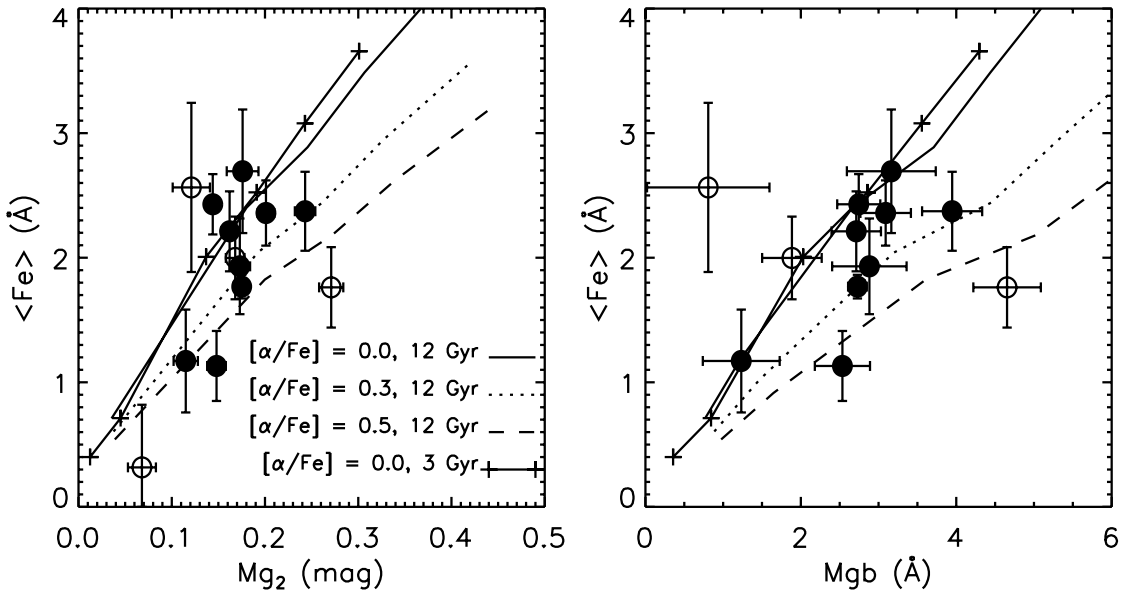

FIG. 6.—⟨Fe⟩ vs. Mg_2 and Mg b, compared with α-enhanced SSP models by TMB02

disturbed morphology, etc.). Although it does have a kinematically decoupled core (KDC), Davies et al. (2001) found no age differences between the KDC and the remainder of the galaxy, and both components appear to have the same elevated Mg-to-Fe ratio. An intermediate-age population may still exist within the central $\sim 1''$ of the nucleus, but its luminosity and associated mass are probably much smaller than required to account for the intermediate-age GCs (Carollo et al. 1997). Even if the KDC indicates a merger history, it is therefore not clear that the event that produced the KDC is related to the origin of the intermediate-age GCs.

In present-day starbursts, formation of clusters is generally accompanied by formation of field stars, so it would be natural to expect a stellar population with the same age and metallicity as the GCs. Indeed, the metallicity of the metal-rich GCs in many systems tends to correlate with that of the parent galaxy (Forbes, Brodie, & Grillmair 1997), suggesting a common origin. If the old age of the general stellar population in NGC 4365 and the intermediate age of the metal-rich GCs are both confirmed, an interesting question will be whether or not there are any field stars associated with the intermediate-age GCs at all. One possibility is that some intermediate-age field stars do exist in NGC 4365 but constitute a too-small fraction of the total population to strongly influence the integrated light.

How many young stars could be hidden in NGC 4365 without significantly affecting the integrated light? A detailed answer to this question is beyond the scope of the present paper, but we can make some rough estimates. First, it is important to specify the age of the young population because the Balmer line strengths and luminosity per unit mass both increase strongly at younger ages, causing even a small number of very young stars to have a strong impact on the integrated spectrum. In a realistic modeling, the effects of different metallicities also need to be considered. However, here we are mainly interested in the *change* in Balmer line strengths in the presence of young stars, and, for this purpose, the metallicity effects can, at least as a first approximation, be considered second order. In the following, we will simply assume solar metallicity. The Maraston SSP models that we have used in previous sections do not tabulate mass-to-light ratios, so for this purpose, we use models by G. Bruzual and S. Charlot (2000, private communication). These models give M/L ratios for various broadband filters, of which we will use the B-band numbers as the best approximation to the region around Hβ. For 2 and 5 Gyr populations, the B-band luminosities per unit mass are about 9.5 and 3.3 times higher than at 15 Gyr, respectively, assuming a Miller-Scalo initial mass function. For solar metallicity, the TMB02 models predict an Hβ equivalent width (EW) of 2.91, 2.16, and 1.51 Å at 2, 5, and 15 Gyr, respectively.

We can now estimate the Hβ EW for any mix of the 2, 5, and 15 Gyr populations by properly weighting each component. For a 15 Gyr population mixed with a 5 Gyr population constituting 5% of the total mass, the Hβ EW is 1.61 Å, about 0.1 Å more than for a pure 15 Gyr population. According to the TMB02 models, this corresponds to an age of 13 Gyr instead of 15 Gyr inferred from the integrated spectrum. If the 15 Gyr population is mixed with a 2 Gyr population, again constituting 5% of the mass, the Hβ EW would increase to 1.98 Å, corresponding to an age of 7 Gyr instead of 15 Gyr. In order to limit the increase in Hβ to 0.1 Å, only about 1% of the mass could be in the 2 Gyr population. For the other Balmer lines, we find very similar results.

While in reality the effects of different metallicities, IMFs, changes in integrated colors, etc. need to be investigated in a more rigorous way, it is clear that only a small number of younger stars could be present in NGC 4365 without noticeable effects on the integrated spectrum. The above considerations suggest that a mass fraction of 1%–5% in a 2–5 Gyr population would lead to a decrease of about 2 Gyr in the luminosity-weighted age estimates (based on Balmer lines), and thus a mass fraction of this order could plausibly remain undetected. It is important to point out, however, that this calculation applies to the integrated light at any given position within the galaxy. If, for example, the young

population was more centrally concentrated, its relative contribution to the mass would have to remain below a few percent even within the central regions and thus constitute a much smaller fraction of the total mass globally.

With current data, the relative numbers of intermediate-age and old *clusters* are poorly constrained, but P02 estimated that about 150 clusters in NGC 4365 (out of a total ~2500; Ashman & Zepf 1998) might belong to the younger population. This corresponds to about 6% of the clusters being young. While the formation efficiency of clusters relative to field stars might vary for the different populations, it is conceivable that any field stars associated with the intermediate-age clusters could be hidden, with the requirement that these stars are uniformly distributed throughout the galaxy. P02 also estimated that 40%–80% of the clusters in their *observed* sample (i.e., within a $2\farcm5 \times 2\farcm5$ field near the center) are young, but because of their color-dependent detection limit, they estimate a biasing factor of 1.8 in the detected numbers of metal-rich (IR-bright) versus metal-poor clusters. However, even a mass fraction as high as ~25% in 2–5 Gyr old field stars in the central regions would completely dominate the integrated spectrum and is clearly incompatible with a uniformly old luminosity-weighted age. The relative numbers of globular clusters and field stars at different metallicities have been examined in detail only for one large elliptical galaxy, the nearby NGC 5128 (Harris & Harris 2002), where the number of clusters relative to field stars seems to *decrease* with increasing metallicity. This trend, then, is the opposite of what would be required in NGC 4365. Both the GC system of NGC 4365 and the field star population clearly warrant further study.

6. SUMMARY

We have presented spectroscopy for 14 globular clusters in NGC 4365, of which nine were suspected to be intermediate-age, metal-rich objects based on *K*-band and optical photometry. Our spectroscopy supports this suspicion for most of the objects, and comparison with current simple stellar population models suggests ages of 2–5 Gyr and metallicities in the range $-0.4 \lesssim [Z/H] \lesssim 0$. However, some old (~10–15 Gyr) clusters are also present. Our spectra thus appear to support the idea that the apparent unimodal optical GC color distribution in NGC 4365 is due to a particular combination of GC ages and metallicities. We see hints of a decrease in $[\alpha/\mathrm{Fe}]$ abundance ratios with increasing metallicity, with close to solar $[\alpha/\mathrm{Fe}]$ for the metal-rich, intermediate-age clusters. The results on GC ages are puzzling in the context of recent data for NGC 4365 itself that suggest that the stellar population is uniformly old with an age of ~14 Gyr. At most, a few percent of the mass could be in a 2–5 Gyr old stellar population without strongly affecting the integrated spectrum. It would be highly desirable with spectroscopy and/or infrared imaging of many more clusters in NGC 4365 in order to better constrain the relative numbers of intermediate-age and old clusters. If confirmed, these findings would pose a significant challenge for understanding the origin of GC subpopulations.

This work was supported by National Science Foundation grants AST 99-00732 and AST 02-06139. We are grateful to C. Maraston and D. Thomas for providing us with their SSP models and to an anonymous referee for helpful comments.

REFERENCES

Ashman, K. M., & Zepf, S. E. 1998, in Cambridge Astrophys. Ser., Globular Cluster Systems (Cambridge: Cambridge Univ. Press)
Barbier-Brossat, M., & Figon, P. 2000, A&AS, 142, 217
Cardelli, J. A., Clayton, G. C., & Mathis, J. S. 1989, ApJ, 345, 245
Carollo, C. M., Franx, M., Illingworth, G. D., & Forbes, D. A. 1997, ApJ, 481, 710
Davies, R. L., et al. 2001, ApJ, 548, L33
de Vaucouleurs, G., de Vaucouleurs, A., Corwin, H. G., Buta, R. J., Paturel, G., & Fouqué, P. 1991, Third Reference Catalogue of Bright Galaxies (New York: Springer)
Faber, S. M., Friel, E. D., Burstein, D., & Gaskell, C. M. 1985, ApJS, 57, 711
Forbes, D. A., Brodie, J. P., & Grillmair, C. J. 1997, AJ, 113, 1652
Forbes, D. A., Franx, M., Illingworth, G. D., & Carollo, C. M. 1996, ApJ, 467, 126
Gebhardt, K., & Kissler-Patig, M. 1999, AJ, 118, 1526
González, J. J. 1993, Ph.D. thesis, Univ. of California, Santa Cruz
Goudfrooij, P., Alonso, M. V., Maraston, C., & Minniti, D. 2001, MNRAS, 328, 237
Harris, W. E., & Harris, G. L. H. 2002, AJ, 123, 3108
Jones, L. A. 1999, Ph.D. thesis, Univ. of North Carolina
Kissler-Patig, M., Brodie, J. P., Schroder, L. L., Forbes, D. A., Grillmair, C. J., & Huchra, J. P. 1998, AJ, 115, 105
Kundu, A., & Whitmore, B. C. 2001, AJ, 121, 2950
Kuntschner, H. 2000, MNRAS, 315, 184
Kuntschner, H., & Davies, R. L. 1998, MNRAS, 295, L29
Larsen, S. S., & Brodie, J. P. 2002, AJ, 123, 1488
Larsen, S. S., Brodie, J. P., Huchra, J. P., Forbes, D. A., & Grillmair, C. 2001, AJ, 121, 2974
Lee, H.-C., Lee, Y.-W., & Gibson, B. K. 2002, in Extragalactic Globular Cluster Systens, ed. M. Kissler-Patig (Berlin: Springer)
Maraston, C., Greggio, L., Renzini, A., Ortolani, S., Saglia, R. P., Puzia, T. H., & Kissler-Patig, M. 2003, A&A, in press
Massey, P., Strobel, K., Barnes, J. V., & Anderson, E. 1988, ApJ, 328, 315
Oke, J. B., et al. 1995, PASP, 107, 375
Puzia, T. H., Zepf, S. E., Kissler-Patig, M., Hilker, M., Minniti, D., & Goudfrooij, P. 2002, A&A, 391, 453
Schiavon, R. P., Faber, S. M., Rose, J. A., & Castilho, B. V. 2002, ApJ, 580, 873
Schlegel, D. J., Finkbeiner, D. P., & Davis, M. 1998, ApJ, 500, 525
Surma, P., & Bender, R. 1995, A&A, 298, 405
Thomas, D., Greggio, L., & Bender, R. 1999, MNRAS, 302, 537
Thomas, D., Maraston, C., & Bender, R. 2003, MNRAS, in press
Tripicco, M. J., & Bell, R. A. 1995, AJ, 110, 3035
Worthey, G., Faber, S. M., González, J. J., & Burstein, D. 1994, ApJS, 94, 687
Worthey, G., & Ottaviani, D. L. 1997, ApJS, 111, 377